PROCEEDINGS of the
23rd International Congress on Acoustics
9 to 13 September 2019 in Aachen, Germany

On the estimation of the damping loss factor of highly damped structures

Mathias HINZ[(1)], Guido SANTOS[(1)], José Vitor MONTEIRO[(1)], Júlio CORDIOLI[(1)], Israel PEREIRA[(2)], Sideto FUTATSUGI[(2)]

[(1)]Vibration and Acoustics Laboratory, Federal University of Santa Catarina, Brazil, julio.cordioli@ufsc.br
[(2)]Smart Structures, Noise and Vibration R&D - EMBRAER, Brazil, israel.pereira@embraer.com.br

Abstract

The damping loss factor (DLF) of a structure represents numerically its power dissipation capacity under a given excitation field, and it is an important input parameter for numerical models based on Statistical Energy Analysis (SEA). Different experimental approaches are described in the literature to obtain the DLF from complex structures. Nevertheless, the application of such methods to estimate the DLF of highly damped structures, for example fuselage panels with viscoelastic materials, may be questionable. With its focus on the DLF computation for highly damped structures, this paper intends to present a broad overview through a numerical-experimental approach on three of the main methods presented in literature: the Power Input Method (PIM), the Periodic Structures Theory and the Inhomogeneous Wave Correlation (IWC). Numerical and experimental results are presented and discussed, exploring details, advantages and limitations according to each method proposed.

Keywords: Viscoelasticity, Fuselage panels, Inhomogeneous Wave Correlation

1 INTRODUCTION

The attenuation of structural vibration is a crucial step during the design of a high performance structure like an aircraft, as it directly impacts the cabin interior noise and vibration levels. As a result, passive damping treatments such as viscoelastic materials (VEM) are widely used due to its simplicity regarding manufacturing/assembly procedures as well as the cost-efficiency relation obtained with such a solution. The VEM application to resonant components, such as the skin of an aircraft fuselage, intensifies the energy dissipation through a vibration cycle (excited, for example, by pressure fluctuations on the turbulent boundary layer), reducing the total amount of energy transmitted vibroacoustically to the airplane interior.

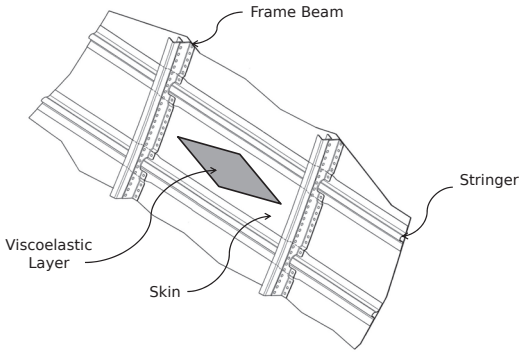

Figure 1. Viscoelastic layer applied to a fuselage panel. [1]

The damping loss factor (DLF) is then the parameter used to quantify the amount of energy dissipated by a given structure under an excitation (mechanical or acoustic) field. Many are the techniques developed with the goal of computing the overall damping loss factor of complex structures.

This paper intends to evaluate three of the most widespread methodologies for damping loss factor estimation, focusing on their main limitations for highly damped cases, recurrent in structures treated with VEM. Therefore, a brief review for the methods implemented is first introduced. Then, numerical and experimental results are discussed for the case of a simple flat plate treated with VEM, seeking to illustrate the difference in the behavior between light and heavily damped structures and how it affects each method. Finally, all the methods are implemented and analyzed for a fuselage panel, also treated with VEM.

2 DAMPING LOSS FACTOR COMPUTATION METHODS

2.1 Power Input Method (PIM)

The definition for a structure's loss factor is given by the ratio between the dissipated energy per oscillation radian ($E_{diss}/2\pi$) and the total reversible energy of the system (E_{vib}) [2]:

$$\eta = \frac{E_{diss}}{2\pi E_{vib}} = \frac{P_{diss}}{\omega E_{vib}}. \tag{1}$$

For the case of steady state conditions, the total power injected (P_{in}) in the system is equal to the amount of power being dissipated. For a random excitation signal, this is given by:

$$P_{in} = P_{diss} = \frac{1}{2\pi}\int_{-\infty}^{\infty} Re\{Y_{ff}(\omega)\}S_{F_fF_f}(\omega)d\omega \tag{2}$$

where $Re\{Y_{ff}\}$ is the real part of the driving point mobility function. $S_{F_fF_f}$ is the force power spectral density on the same point.

Now, we recall that the vibrational energy is the sum of the kinetic and elastic energies.

$$E_r = E_k + E_u \tag{3}$$

According to SEA hypothesis, when the structure is submitted to a stationary white noise force, as long as a diffuse field is established, the expectations of kinetic and elastic energies are equal [3]

$$< E_k > = < E_u > \tag{4}$$

and the vibrational energy is then given by Equation 5

$$E_r = 2E_k \tag{5}$$

where the kinetic energy is chosen since it is easier to measure than the elastic energy experimentally and numerically. One must notice that highly damped structures will likely fail to meet the diffuse field condition, as the waves will be dissipated before reaching the boundaries. The diffuse field hypothesis leads to:

$$2E_k = \int_V \rho \frac{1}{2\pi}\int_{-\infty}^{\infty} S_{v_iv_i}(\omega)d\omega dV \tag{6}$$

where ρ is the material density, V its volume and $S_{v_iv_i}$ is the velocity power spectral density function for each point i being measured.

Combining Equations 2 e 6 into Equation 1, and performing some manipulations [1], one can find the final expression for the loss factor (η) computation, given by:

$$\eta(\omega) = \frac{Re\{Y_{ff}(\omega)\}}{\omega\sum_{i=1}^{N} m_i|Y_{if}(\omega)|^2} \tag{7}$$

The equation above is the one commonly used for experimental/numerical computation when implementing the PIM theory. The procedure is simply developed by segmenting the complete structure in discrete elements (representing the masses m_i) and measuring the driving and transfer mobility functions in Equation 7.

2.2 Periodic Structures Theory

When discussing numerical models, the Periodic Structures theory presents an interesting alternative to the conventional full FEM approach, when taking into account space periodicity of a given structure, represented by the repetition of a cell [4].

Given this, one can propose a relationship between the structure's degrees of freedom (DOF) as a function of the wavenumbers (k_x e k_y) and nodes' distances given by the relation:

$$\mathbf{q}' = \mathbf{P}(k_x, k_y)\mathbf{q} \tag{8}$$

where the periodicity matrix $\mathbf{P}$ summarizes this relationships between the original DOF vector $\mathbf{q}$ and a reduced array $\mathbf{q}'$. With this considered, one can write the equation of motion for the given cell (considering as well the periodicity for the internal forces) as:

$$\mathbf{P}^H(\mathbf{K} - \omega^2\mathbf{M})\mathbf{P}\ \mathbf{q}' = \mathbf{P}^H\mathbf{F} = 0 \tag{9}$$

where $\mathbf{P}^H$ is the hermitian of $\mathbf{P}$. $\mathbf{M}$ and $\mathbf{K}$ are the original mass and stiffness matrices for the cell. The final equation is then written as:

$$(\bar{\mathbf{K}}(k_x, k_y) - \omega^2\bar{\mathbf{M}}(k_x, k_y))\ \mathbf{q}' = 0 \tag{10}$$

For structural damping, the dissipated power is proportional to the local strain energy on the element (U_r). Considering local loss factors (η_r) for the different regions on the structure being analyzed, the total dissipated power is given by

$$P_{diss} = \sum_r 2\omega\eta_r U_r \tag{11}$$

The total and strain energies can, finally, be expressed in terms of stiffness and mass matrices and the wave mode, given by the eigenvector (ϕ_n) obtained as a solution to Equation 10. Therefore, the loss factor for a given wave n is given by:

$$\eta_n = \frac{\sum_r 2\eta_r \phi_n^H \bar{K}_r \phi_n}{\phi_n^H[\bar{K} + \omega^2\bar{M}]\phi_n} \tag{12}$$

The final step is then the computation of an average loss factor for a given frequency band. Assuming a reverberant diffuse field, the structure loss factor can be computed as an average of Equation 12 over all the wavenumber values whose natural frequencies lie within the band of interest.

2.3 Inhomogeneous Wave Correlation (IWC)

The IWC method [5] is based on the measurement of the correlation between harmonic displacement fields. For a fixed frequency (ω), a 2D harmonic displacement field ($\hat{w}$) obtained from the desired structure is selected to be a reference, compared with the harmonic field generated by a inhomogeneous wave (Equation 13).

$$\hat{\varphi}_{k,\gamma,\theta}(x, y) = e^{ik(1+i\gamma)(xcos\theta + ysin\theta)} = e^{i\tilde{k}(xcos\theta + ysin\theta)} \tag{13}$$

First, the heading angle (θ) of the inhomogeneous wave is fixed, and multiple values of the wavenumber k and the attenuation factor γ are iterated, creating several harmonic fields depending on the selected pair (k_{it}, γ_{it}).

Then, the Modal Assurance Criterion [6] (Equation 14) is applied to quantitatively compare how similar is the shape of each inhomogeneous wave displacement field ($\hat{\varphi}(k_{it}, \gamma_{it})$) and the reference one ($\hat{w}$).

$$IWC(k, \gamma, \theta) = \frac{\left|\sum_N \hat{w}(x_i, y_i).\hat{\varphi}^*_{k,\gamma,\theta}(x_i, y_i)\Delta S_i\right|}{\sqrt{\sum_N |\hat{w}(x_i, y_i)|^2 \Delta S_i . \sum_N |\hat{\varphi}_{k,\gamma,\theta}(x_i, y_i)|^2 \Delta S_i}} \tag{14}$$

where $\hat{}$ represents ω dependence and * the complex conjugate. S_i is the equivalent area for the measurement point and N is total measured points.

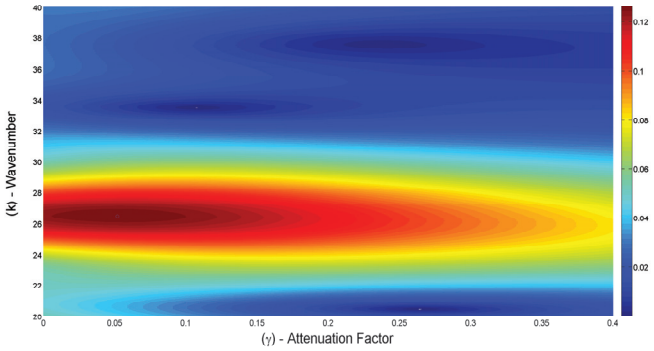

Figure 2. Example of IWC(k,γ) mapping for a fixed θ.

The processes is then repeated fixing now different values θ, selecting for each heading angle the best correlation found by the IWC equation.

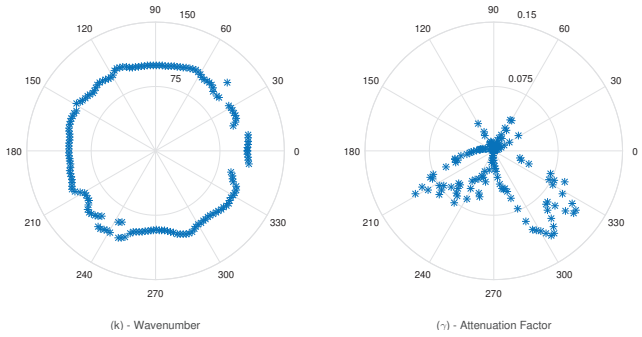

Figure 3. Example of pairs of k and γ selected for each θ of a frequency ω.

Once the previous steps were performed for all the 2D harmonic displacement fields ($\hat{w}$) (one for each ω), the damping loss factor can be then computed from Equation 15. [7]

$$\eta(\omega) = \left| \frac{Im(\tilde{k}^4)}{Re(\tilde{k}^4)} \right| \tag{15}$$

3 IMPLEMENTATION

3.1 Case 1 - Numerical flat plate

The first case consists of retrieving the harmonic displacement fields from a numerical model developed in the software VA One ®, for a simple flat plate considering three different cases of damping.

- *Dimensions* $\rightarrow L \times W \times t = 0,5 \times 0,35 \times 0,0012m$
- *Density* $\rightarrow \rho = 2700 \frac{kg}{m^3}$
- *Young and Shear moduli* $\rightarrow E' = 71GPa \ \& \ G' = 26,7GPa$
- *Frequency range* $\rightarrow f = 50 - 1 - 5600Hz$
- *Damping Loss factors* $\rightarrow \eta_1 = 0,01; \eta_2 = 0,1; \eta_3 = 0,3$

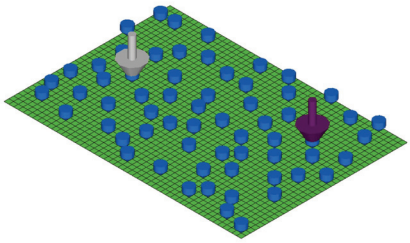

Figure 4. PIM - *2 Forces / 64 Acquisition Points*

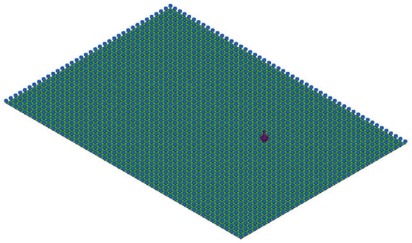

Figure 5. IWC - *1 Force / 1836 Acquisition Points (Full mesh)*

3.2 Case 2 - Experimental flat plate with periodic VEM

The second case is again an aluminum flat plate, now considering two different setups of a periodically attached VEM. The first one presents a 25% VEM coverage, while the second, 50%. The mobilities in this case were measured using a laser vibrometer (Polytec® PSV-500).

- *Dimensions* $\rightarrow L \times W \times t = 0,5 \times 0,35 \times 0,0012m$
- *Frequency range* $\rightarrow f = 50 - 2 - 12800Hz$
- *Acquisition Points* $\rightarrow 493$

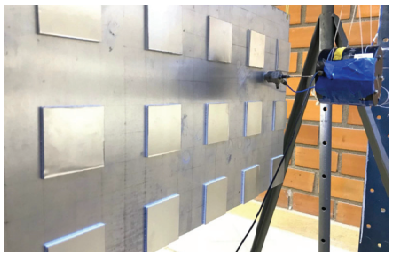

Figure 6. 25% coverage.

Figure 7. 50% coverage.

Beyond the experimental procedure, results for the mobilities were also calculated through numerical models of such configurations, using equivalent properties obtained experimentally [8] to characterize the areas with VEM application. The FEM model was implemented through Nastran®, while the periodic structure method was implemented through VA One®, taking into account the geometry pattern used in the specimen measured.

3.3 Case 3 - Fuselage Panel with VEM

The third case is a fuselage panel with stringers and frames configured to create a 4x6 cell structure. The fuselage panel skin is covered with VEM in constrained form, covering approximately 50% of the total inner area. For this case, as in the last one, the mobilities were measured using a laser vibrometer (Polytec® PSV-500).

- *Dimensions* $\rightarrow L \times W = 1.8 \times 1.13m$
- *Frequency range* $\rightarrow f = 50 - 10000Hz$
- *Acquisition Points* $\rightarrow 451$

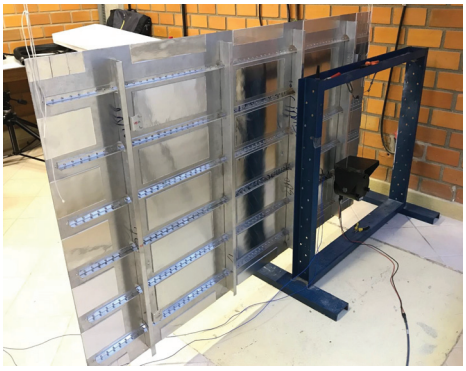

Figure 8. VEM disposition on the Panel.

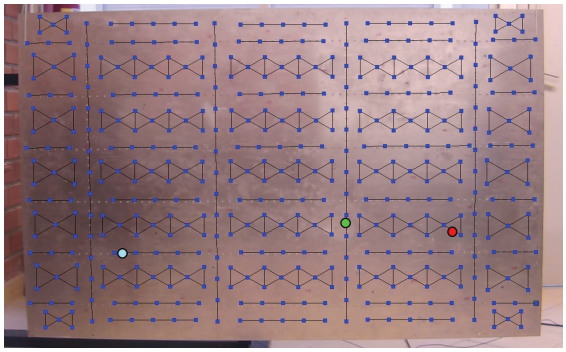

Figure 9. Excitation (Beam - blue , Stringer - green, Skin - red) and Acquisition nodes.

As in the flat plate with periodic VEM, the properties of the applied VEM area were obtained experimentally to supply the numerical models. A FEM model was then built on Nastran® software, while the periodic structure method was applied in VA One®, taking into account one cell of the fuselage panel.

4 RESULTS AND FURTHER DISCUSSIONS

4.1 Case 1

Figure 10 shows the damping loss factor estimations for three scenarios of DLF ($\eta_1 = 0,01$, $\eta_2 = 0,1$ and $\eta_3 = 0,3$, constant in frequency) used as input for the flat plate FEM model in VA One®

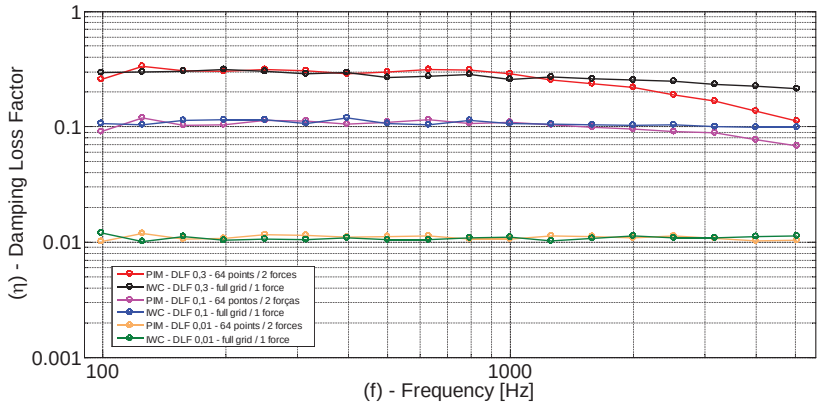

Figure 10. DLF estimation for $\eta_1 = 0,01$, $\eta_2 = 0,1$ and $\eta_3 = 0,3$.

It becomes clear that for cases categorized as low and moderate damping (η_1 e η_2), results for the two methods converge quite well to the input result. Nevertheless, for the high damping scenario (η_3), the results for the PIM start to diverge with a frequency increase. One observes that this behavior is based on the fact previously stated that the reverberant field gradually disappears for higher frequencies as all the energy is dissipated before the wave can reach the boundaries, as illustrated in Figures 11 and 12, where reverberant and direct fields are respectively dominants. One can finally observe that the IWC was the method with the closest results to the expectations for the highly damped model.

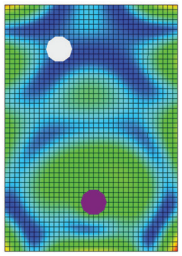

Figure 11. Displacement field for $f = 200Hz$.

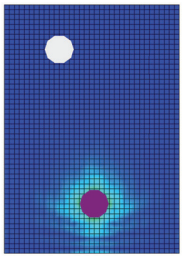

Figure 12. Displacement field for $f = 5000Hz$.

4.2 Case 2

Figures 13 and 14 illustrate, respectively, loss factor estimates for the two different VEM coverage cases (25% and 50%). All the results present a good agreement, which indicates that the added damping caused by the VEM treatment was not enough to cause a direct field predominance, which would affect the PIM results.

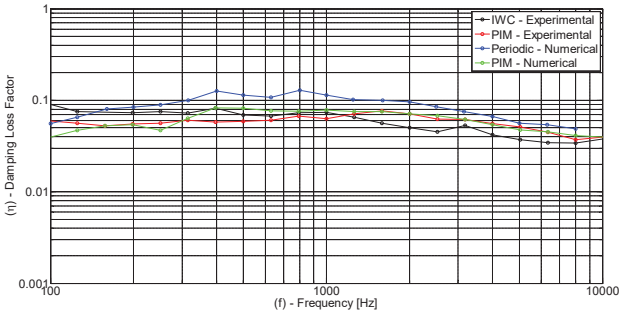

Figure 13. DLF estimation for 25% coverage.

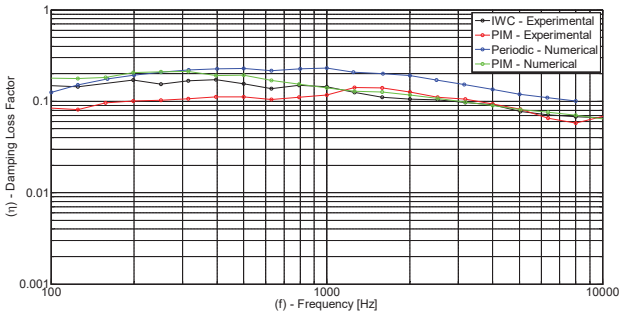

Figure 14. DLF estimation for 50% coverage.

4.3 Case 3

Figure 15 shows the fuselage panel loss factor estimation for both numerical and experimental analyses. The results show a very good convergence between themselves, for both numerical and experimental data, with PIM and IWC capturing the same behavior inside a small margin of variation. Again, the application o VEM covering nearly 50% of the skin of a fuselage panel still didn't reach a state of dominance of the direct field, which would lead the PIM to failure.

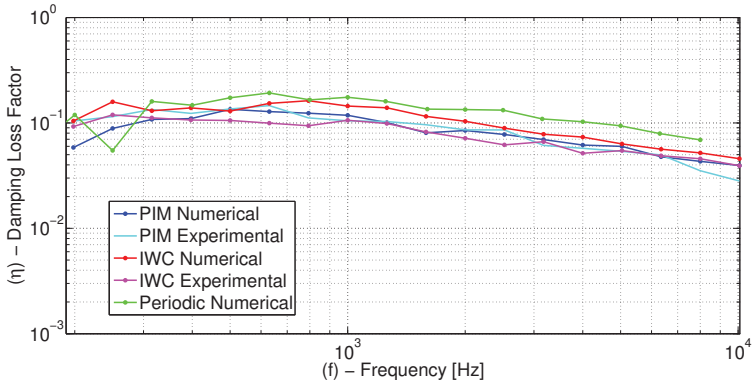

Figure 15. DLF estimation for fuselage panel.

5 CONCLUSIONS

The purpose of this paper was to evaluate and compare different methodologies for loss factor estimation in complex damped structures. While the PIM showed to be a very simple and fast way of computing the DLF, it might fail in critical cases where the dissipation is so high that there is no reflection of waves in the structure, failing this way the diffuse field assumption.

In the other hand, the IWC presented good results when compared to those obtained by the traditional methods, not presenting any limitation for high values of damping. However, although the IWC method may present advantages, it has also its own limitations. Among them, it is possible to emphasize the necessity to use a relatively complex and expensive system of measurement as the laser scanning, as well as the high computational cost to handle the calculation and analyze the results when compared to other methods.

REFERENCES

[1] Hinz, M. Numerical evaluation of damping loss factor estimation techniques for sheet metal structures. Trabalho de Conclusão de Curso, Universidade Federal de Santa Catarina, Florianópolis, 2018.

[2] Cremer, L.; Heckl, M.; Petersson, B. Structure-Borne Sound: Structural Vibrations and Sound Radiation at Audio Frequencies, Springer Verlag, Berlin, 2005.

[3] Le Boat, A. Foundation of Statistical Energy Analysis in Vibroacoustics, OUP Oxford, Lyon, 2015.

[4] Cotoni, V.; Langley, R.; Shorter P. A statistical energy analysis subsystem formulation using finite element and periodic structure theory. Journal of Sound and Vibration, 318:1077-1108, 2008.

[5] Berhaut, J. Contribution a l'identification large bande des structures anisotropes: application aux tables d'harmonie des pianos. Thèse de Doctorat, Ecole Centrale de Lyon, Lyon, 2004.

[6] Ewins, D. Modal Testing: Theory and Practice, Research Studies Press Letchworth, London, 1984.

[7] Cherif, R.; Chazot, J.; Atalla, N. Damping loss factor estimation of two-dimensional orthotropic structures from a displacement field measurement. Journal of Sound and Vibration, 356:61-71,2015.

[8] Santos, G. Determinação do amortecimento de painéis aeronáuticos a partir da caracterização dinâmica de materiais viscoelásticos via ajuste de modelo. Dissertação de Mestrado, Universidade Federal de Santa Catarina, Florianópolis, 2019.